Shock detection and limiting strategies for high order discontinuous Galerkin schemes

C. Altmann, A. Taube, G. Gassner, F. Lörcher, and C.-D. Munz

IAG - Institut für Aerodynamik und Gasdynamik, Universität Stuttgart, Pfaffenwaldring 21, 70569 Stuttgart Germany

1 Introduction

Discontinuous Galerkin (DG) schemes are a combination of finite volume (FV) and finite element (FE) schemes. While the approximate solution is a continuous polynomial in every grid cell, discontinuities at the grid cell interfaces are allowed which enables the resolution of strong gradients. How to calculate the fluxes between the grid cells and to take into account the jumps is well-known from the finite volume community. Due to their interior grid cell resolution with high order polynomials the DG schemes may use very coarse grids. In this approach the cumbersome reconstruction step of finite volume schemes is avoided, but for every degree of freedom a variational equation has to be solved. The main advantage of DG schemes is that the high order accuracy is preserved even on distorted and irregular grids. In the following we present a DG scheme based on a space-time expansion (STE-DG), which was proposed in [4]. Our scheme features *time consistent* local time-stepping, where every grid cell runs with its optimal time step.

An open issue for DG schemes in general is an efficient shock-capturing strategy. The very successful FV shock-capturing consists of a TVD or WENO reconstruction which is non-oscillatory. In combination with local grid refinement a narrow transition zone at the shock wave is obtained within ~ 4 grid cells. This can also be extended to DG schemes in a way such that the trial function is locally replaced by a reconstructed polynomial. As the efficiency of our STE-DG scheme relies on the locality of the spatial discretization, the use of this shock-capturing technique is cumbersome, especially for high order. Another approach which is more convenient for DG schemes is to keep the large grid cell and to resolve the shock within the grid cell by a narrow viscous profile by locally adding some sort of artificial viscosity. This was recently proposed by Persson and Peraire [5]. Their approach is quite contradictory to FV shock-capturing, since here the order of accuracy is kept high or is even increased locally. Persson and Peraire showed that this strategy captures the shock within a transition zone the size of $\delta = \frac{4h}{p+1}$ where p denotes the degree of the polynomial approximation. In this case the shock profile can be sharpened by increasing the degree of the trial function (p-adaptation). While Persson and Peraire applied this shock-capturing by p-refinement within an implicit scheme, we combine it with an explicit scheme which leads to an anisotropic time step distribution due to the stability restriction. But, due to our local time-stepping feature the efficiency is well preserved.

2 The STE-DG scheme for the Euler equations

2.1 The equations and the semi-discrete variational formulation

The Euler equations in two space dimensions read as

$$\mathbf{U}_t + \mathbf{F}\left(\mathbf{U}\right)_x + \mathbf{G}\left(\mathbf{U}\right)_y = \mathbf{0} \tag{1}$$

with

$$\mathbf{U} = \begin{pmatrix} \rho \\ \rho u \\ \rho v \\ \rho e \end{pmatrix}, \quad \mathbf{F} = \begin{pmatrix} \rho u \\ \rho u^2 + p \\ \rho uv \\ \rho u(e+p) \end{pmatrix}, \quad \mathbf{G} = \begin{pmatrix} \rho v \\ \rho uv \\ \rho v^2 + p \\ \rho v(e+p) \end{pmatrix}, \tag{2}$$

where ρ, u, v, p, and e denote the density, x- and y-velocity, pressure, and specific total energy, respectively. We consider the equation of state of a perfect gas with

$$p = \rho RT = (\gamma - 1)\rho\epsilon \quad \text{and} \quad e = \frac{p}{(\gamma-1)\rho} + \frac{u^2+v^2}{2}, \tag{3}$$

where ϵ denotes the specific internal energy, γ is the isentropic exponent, and R is the gas constant.

The spatial discretization is based on the weak formulation of equation (1). We multiply the Euler equations with an arbitrary test function $\mathbf{\Phi}(\mathbf{x})$, integrate over the grid cell Q_i and use integration by parts for the flux terms to get

$$\int_{Q_i} \mathbf{U}_t \cdot \mathbf{\Phi}\, dx + \int_{\partial Q_i} \mathbf{F}_n \cdot \mathbf{\Phi}\, ds - \int_{Q_i} \left(\mathbf{F}\cdot\mathbf{\Phi}_x + \mathbf{G}\cdot\mathbf{\Phi}_y\right) dx = 0, \tag{4}$$

where ∂Q_i denotes the surface of the grid cell and $\mathbf{F}_n$ is normal component of the flux.

To get the semi-discrete DG scheme we introduce a piecewise polynomial approximation $U_h(\mathbf{x}, t)$, which is defined as

$$U_i(\mathbf{x}, t) := \sum_{l=1}^{N(p)} \hat{\mathbf{U}}_l^i(t)\, \varphi_l(\mathbf{x}) \tag{5}$$

in every grid cell Q_i. Using a trial space of piecewise polynomials with a degree $\leq p$, we can introduce an orthonormal basis $\{\varphi\}_{l=1}^{N(p)}$, where $N(p) = (p+1)(p+2)/2$ in two space dimensions. We choose as test functions the basis functions and get the following $N(p)$ ordinary differential equations for the $N(p)$ unknowns

$$(\hat{U}_l^i)_t = -\int_{\partial Q_i} \mathbf{H}\cdot\boldsymbol{\varphi}_l\, ds + \int_{Q_i} \mathbf{F}\cdot(\boldsymbol{\varphi}_l)_x + \mathbf{G}\cdot(\boldsymbol{\varphi}_l)_y\, dx = 0, \quad l = 1, ..., N(p). \tag{6}$$

As numerical flux we use the HLLC flux (see, e.g., [1]) named $\mathbf{H}$.

2.2 The space-time expansion approach with local time-stepping

For the STE-approach the semi discrete scheme (6) is simply integrated in time. Due to the local time stepping, we give up the assumption that all grid cells run with the same

time step and therefore we do not have any longer a common time level. Let us denote the actual local time level in grid cell Q_i by t_i^n. The degrees of freedom $\hat{\mathbf{U}}_l^{i,n}$ represent the solution at t_i^n in this grid cell. Furthermore, each cell may evolve in time with its local time step Δt_i^n which has to satisfy the local stability restriction, which depends on the grid cell diameter as well as on the order $p+1$, see [4]. With Δt_i^n, the next local time level in Q_i is given as

$$t_i^{n+1} = t_i^n + \Delta t_i^n. \tag{7}$$

The evolution equations for the degrees of freedom read as

$$\hat{U}_l^{i,n+1} = \hat{U}_l^{i,n} - \int\limits_{\partial Q_i} \mathbf{H} \cdot \boldsymbol{\varphi}_l \, ds + \int\limits_{Q_i} \mathbf{F} \cdot (\boldsymbol{\varphi}_l)_x + \mathbf{G} \cdot (\boldsymbol{\varphi}_l)_y \, dx = 0, \quad l = 1, ..., N(p). \tag{8}$$

To evaluate the right hand side of the evolution equations the space-time integrals are approximated by proper Gaussian integration rules. The difficulty is, that the values at the space-time Gauss points are not known. In the STE-approach a space-time Taylor expansion of the approximation U_i at the grid cell barycenter $\mathbf{x}_i$ at time level t_n

$$\widetilde{\mathbf{U}}_i(x,t) := \sum_{l=0}^{p} ((t - t_i^n)\, \partial_t + (\mathbf{x} - \mathbf{x}_i)\boldsymbol{\nabla})^l U(x,t)|_{\mathbf{x}_i, t_n} \tag{9}$$

is used to get an high order approximation at every space-time Gauss point. While the space derivatives are already available within the DG approach, the mixed space-time derivatives are approximated using the (CK-) Cauchy-Kovalevskaya procedure. To replace the time and mixed space-time derivatives the evolution equation is applied several times, see [4] for more details.

As the evaluation of the fluxes between the grid cells on the right hand side relies on neighbor data as well, the local time-stepping algorithm is based on the following evolve condition: The evolution of the DOF are performed, if

$$t_i^{n+1} \leq \min\left\{t_j^{n+1}\right\}, \forall j : \, Q_j \cap Q_i \neq \emptyset \tag{10}$$

is satisfied. This means that an element can only be updated in time, if all neighboring elements' j prospective time level is bigger than the one from element i in concern. This guarantees that the approximate space-time values of the neighbor cells are available. In this manner, the algorithm continues by searching for elements satisfying the evolve condition (10). So all elements are evolved in a suitable order by evaluating the different terms of the right hand side of equation (8) for each element in an effective order. At each time, the interface fluxes are defined uniquely for both adjacent elements, making the scheme exactly conservative, for more details see [2].

3 Sub-Cell Shock Capturing for DG methods

The first step is to detect grid cells in which a strong gradient is approximated and which will lead to spurious oscillations in the approximative piecewise polynomial. In order to determine a suitable sensor for under-resolved parts, we make use of the fact that the solution within each element is represented in terms of an orthogonal basis

$$\mathbf{U}_i(x,t_n) = \sum_{l=1}^{N(p)} \hat{\mathbf{U}}_l^i \mathbf{\Phi}_l. \tag{11}$$

If the underlying exact solution is smooth, we expect the coefficients of the approximation to decay fast. E.g., using the density ρ from the set of conservative variables we apply as proposed in [5] a smoothness sensor in the form

$$S_i := \frac{\sum_{l=N(p-1)+1}^{N(p)} (\hat{\rho}_l)^2}{\sum_{l=1}^{N(p)} (\hat{\rho}_l)^2}. \tag{12}$$

This expression measures the rate of the decay of the magnitude of the coefficients If this rate is low then we have identified a strong gradient which is not well resolved by the local polynomial, e.g. a shock wave. Once the shock has been sensed, we modify the equation locally in this grid cell by introducing an artificial viscosity of the form

$$\mathbf{U}_t + \mathbf{F}(\mathbf{U})_x + \mathbf{G}(\mathbf{U})_y = \nabla \cdot (\varepsilon \nabla \mathbf{U}). \tag{13}$$

The piecewise constant viscosity ε is chosen as a function of the value S_i of the discontinuity sensor and proportional to the available resolution $\sim \frac{4h_i}{p_i+1}$ within the grid cell, see [5] for details. The discretization of the viscous terms is based on exact diffusive Riemann solutions for parabolic equations, see [2] and [3] for details.

4 Results

This section contains results of one- and two-dimensional test cases to show the properties of the STE-DG scheme with this shock-capturing technique.

4.1 Shock Capturing

To demonstrate the capabilities of the shock capturing method we performed a simple test using a Mach 10 shock moving through the computational domain. In addition to our scheme, we performed for comparison the calculation also with a 4^{th} order WENO reconstructed Finite Volume scheme and a 3^{rd} order DG scheme with HWENO limiting. The shock profiles in density together with the grid sizes after $t = 0.16$ are plotted in figure 1.

The 3^{rd} order DG scheme and the 4^{th} order rec. FV scheme both ran on 100 cells, while for the $\mathcal{O}5$ STE-DG scheme only 25 cells were used. One notices that all profiles look rather similar. As expected the DG HWENO and the rec. FV scheme both smeared the shock over 3 cells as usual for these limiting strategies and schemes, respectively. In contrast, the artificial viscosity limiter was able to capture the profile within one cell with almost the same resolution, but using only 1/4 of the HWENO-DG cells.

If this calculation were performed on the same grid, the artificial viscosity method would produce an even sharper shock profile, and would still be able to resolve the shock within just one cell.

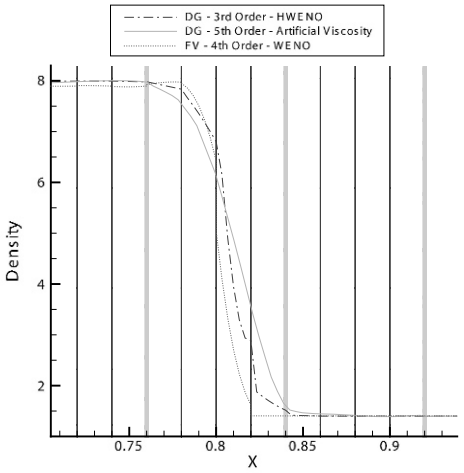

Fig. 1. Comparison of shock capturing properties. Plot of a 3rd order DG scheme, a 4^{th} order WENO reconstructed FV scheme and the 5^{th} order STE-DG scheme with artificial viscosity

4.2 The Double Mach reflection test-case

The Double Mach reflection (DMR) test-case can be considered as a challenging problem for numerical schemes because of different flow phenomena that are lying side by side:

When a Mach 10 shock hits a wedge, a triple-point is formed consisting of two shocks and a slightly unstable contact discontinuity that rolls up at the wedge boundary. To recover the vortex roll-up, the shock capturing has to be performed in a very local way, not affecting the vortices.

Figure 2 shows a density plot of a 6^{th} order calculation as well as a close-up of the triple-point region including some gridcells. One can see that both the shock as well as the vortex are clearly dissolved and - in addition - that the shock profile is captured within only one cell.

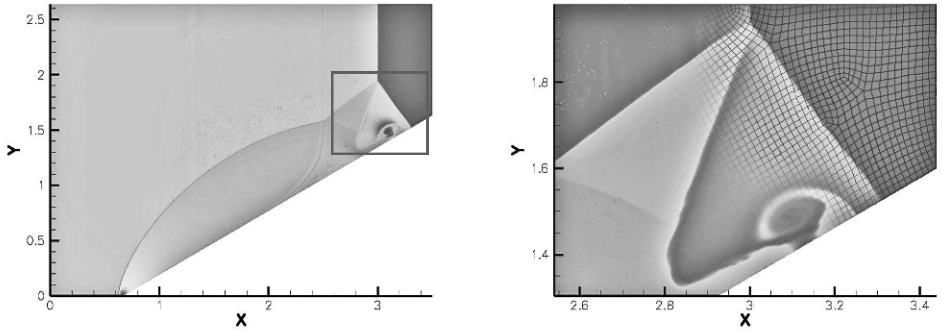

Fig. 2. The double mach reflection problem. Density plot at $t = 0.2$ of the computational domain (left) as well as a zoomed cutout including gridcells (right)

The previously described smoothness sensor and the added viscosity are plotted in figure 3. One can clearly see that viscosity was added only to the strong Mach 10 shock and therefore did not affect the rest of the solution in a bad way.

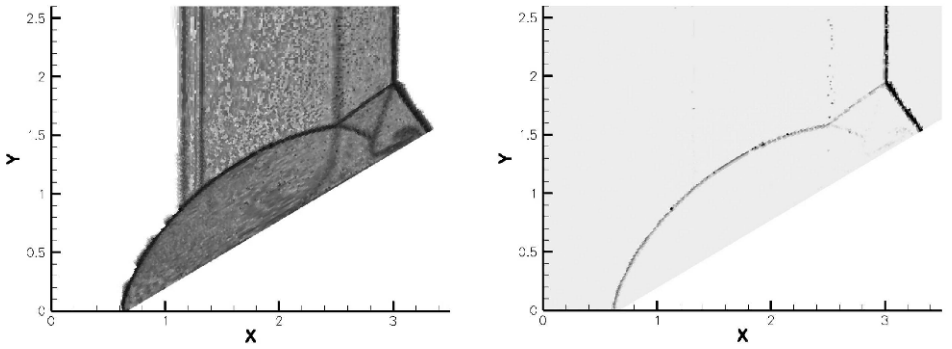

Fig. 3. The double mach reflection problem. Plot of the smoothness sensor (left) and artificial viscosity distribution (right)

5 Conclusion and Outlook

In this paper we combined an explicit space-time DG scheme with the shock-capturing approach of Persson and Peraire [5]. The idea to keep a high order approximation and to add locally artificial viscosity for the subgrid resolution of the shock works also very well also for unsteady problems. To preserve efficiency in the explicit unsteady approach it is essential to use the local time stepping framework.

References

1. E. F. Toro. *Riemann solvers and numerical methods for fluid dynamics.* Springer, second edition, 1999.
2. G. Gassner and F. Lörcher and C.-D. Munz. A Contribution to the Construction of Diffusion Fluxes for Finite Volume and Discontinuous Galerkin Schemes. *J. Comput. Phys.*, 2006. doi:10.1016/j.jcp.2006.11.004.
3. Gassner, G., Lörcher, F., and Munz, C.-D. A discontinuous Galerkin scheme based on a space-time expansion II. Viscous flow equations in multi dimensions. *submitted to Journal of Scientific Computing*, 2006.
4. Lörcher, F., Gassner, G., and Munz, C.-D. A discontinuous Galerkin scheme based on a space-time expansion. I. Inviscid compressible flow in one space dimension. *Journal of Scientific Computing*, 2006. DOI:0.1007/s10915-007-9128-x.
5. Per-Olof Persson and Jaime Peraire. Sub-Cell Shock Capturing for Discontinuous Galerkin Methods. In *Proc. of the 44th AIAA Aerospace Sciences Meeting and Exhibit*, AIAA-2006-1253, Reno, Nevada, January 2006.